Effects of platelet-rich fibrin produced by three centrifugation protocols on bone neoformation in defects created in rat calvaria

Débora de Souza Ferreira Sávio, Lucia Moitrel Pequeno da Silva, Gabriel Guerra David Reis, Ricardo Junior Denardi, Natacha Malu Miranda da Costa, Flávia Aparecida Chaves Furlaneto, Sérgio Luís Scombatti de Souza, Carlos Fernando de Almeida Barros Mourão, Richard J. Miron, Roberta Okamoto & Michel Reis Messora

Published online: 06 Jul 2023.

Submit your article to this journal ↗

View related articles ↗

View Crossmark data ↗

RESEARCH ARTICLE

Check for updates

Effects of platelet-rich fibrin produced by three centrifugation protocols on bone neoformation in defects created in rat calvaria

Débora de Souza Ferreira Sávio [1], Lucia Moitrel Pequeno da Silva [2], Gabriel Guerra David Reis [2], Ricardo Junior Denardi [2], Natacha Malu Miranda da Costa [2], Flávia Aparecida Chaves Furlaneto [2], Sérgio Luís Scombatti de Souza [2], Carlos Fernando de Almeida Barros Mourão [3], Richard J. Miron [4], Roberta Okamoto [5], & Michel Reis Messora [2]

[1]Department of Morphology, Physiology, and Basic Pathology – DMFPB, School of Dentistry of Ribeirão Preto, University of São Paulo – USP, Ribeirão Preto, Brazil, [2]Department of Oral and Maxillofacial Surgery and Periodontology – DCTBMF, School of Dentistry of Ribeirão Preto, University of São Paulo – USP, Ribeirão Preto, Brazil, [3]Department of Periodontology, Tufts University School of Dental Medicine, Boston, MA, USA, [4]Department of Periodontology, University of Bern, Bern, Switzerland, and [5]Department of Basic Sciences - DCB, School of Dentistry of Araçatuba, Paulista State University – UNESP, Araçatuba, Brazil

Abstract

This study evaluated the potential of Leukocyte-platelet-rich fibrin (L-PRF; fixed angle centrifugation protocol), Advanced-platelet-rich fibrin (A-PRF; low-speed fixed angle centrifugation protocol), and Horizontal-platelet-rich fibrin (H-PRF; horizontal centrifugation protocol) in bone neoformation in critical size defects (CSDs) in rat calvaria. Thirty-two rats were divided into groups: Control (C), L-PRF, A-PRF, and H-PRF. 5 mm diameter CSDs were created in the animals' calvaria. Defects from group Control (C) were filled with blood clots, while defects from groups L-PRF, A-PRF, and H-PRF were filled with respective platelet-rich fibrin (PRF) membranes. L-PRF, A-PRF, and H-PRF were prepared from animal blood collection and specific centrifugation protocols. At 14 and 30 days, calcein (CA) and alizarin (AL) injections were performed, respectively. Animals were euthanized at 35 days. Microtomographic, laser confocal microscopy, and histomorphometric analyzes were performed. Data were statistically analyzed (ANOVA, Tukey, $p < .05$). L-PRF, A-PRF, and H-PRF groups showed higher values of bone volume (BV), newly formed bone area (NFBA), and precipitation of CA and AL than the C group ($p < .05$). The H-PRF group showed higher values of BV, number of trabeculae (Tb. N), NFBA, and higher precipitation of AL than the A-PRF and L-PRF groups ($p < .05$). Therefore, it can be concluded that: i) L-PRF, A-PRF, and H-PRF potentiate bone neoformation in CSDs in rat calvaria; ii) H-PRF demonstrated more biological potential for bone healing.

Plain Language Summary

After tooth loss, the alveolar bone (which supports the teeth) undergoes a natural process called bone remodeling, which can lead to significant decreases in bone height and thickness over time. Faced with the need to replace missing teeth, especially when it comes to dental implants, the lack of supporting tissues can compromise their correct positioning, leading to negative impacts on the success and longevity of the treatment. Therefore, over the years, several materials and procedures have been proposed to preserve and regenerate oral tissues. Leukocyte-platelet-rich fibrin (L-PRF) consists of a membrane obtained by centrifuging the patient's blood in a fixed-angle centrifuge, allowing cells to be available to stimulate tissue regeneration directly at the place of action. Several reports demonstrate high potential in stimulating the formation of new tissues using L-PRF. In recent years, new protocols have been proposed to increase cell concentration and improve the regenerative potential of these membranes, changing the speed and time of centrifugation and introducing horizontal centrifugation. However, there still needs to be concrete evidence of the superiority of the new protocols in relation to the original protocol. In this study, we evaluated the healing of defects

created in rat calvaria using platelet aggregates obtained through different centrifugation protocols. Within the limits of this study, it can be concluded that platelet aggregates improve bone healing, and horizontal centrifugation promotes more satisfactory results compared to fixed-angle protocols.

Introduction

One of the biggest challenges of regenerative therapies in Dentistry, especially after the advent of titanium implants, is to replace lost tissues properly or even prevent loss before it occurs so that the introduced treatment results in success and longevity, leading to the search for the development of materials that promote regeneration effectively in defect areas.[1,2]

In this sense, the use of platelet concentrates made from the patient's blood, like the Leukocyte-platelet-rich fibrin (L-PRF), has been proposed in recent years, obtaining an easily applicable three-dimensional membrane with promising results in promoting tissue regeneration. With this concept, it is suggested that cells and growth factors can be collected from the patient and applied to the surgical site to stimulate tissue regeneration.[2–6]

L-PRF consists of a three-dimensional fibrin network, characteristic of the final stages of the coagulation cascade, forming a biological framework that acts as a source of cytokines and growth factors such as platelet-derived growth factor (PDGF), transforming growth factor (TGF)-β, insulin-like growth factor (IGF)-1, fibroblast growth factor (FGF), and vascular endothelial growth (VEGF).[6–14] Thus, it promotes the acceleration of cell migration and proliferation, angiogenesis, modulation of the immune response, and recruitment of undifferentiated mesenchymal cells, which favors the repair and regeneration of soft and hard tissues.[6–14]

Initially proposed for the potentiation of bone neoformation after the installation of dental implants, the use of L-PRF currently extends to periodontal therapies and bone reconstructions, such as grafting procedures and post-extraction socket preservation,[15,16] tissue repair in furcation defects,[17,18] root coverage in gingival recessions,[19–21] and procedures for maxillary sinus lift.[22,23]

In recent years, new protocols for the production of platelet concentrates have been proposed, giving rise to the concepts of centrifugation at reduced speed and time, including Advanced-platelet-rich fibrin (A-PRF) and platelet-rich fibrin (PRF) through horizontal centrifugation (H-PRF) to promote greater retention of platelets and leukocytes and consequently greater release of growth factors, enhancing regenerative and healing effects. *In vitro*, studies have demonstrated better structural characteristics, such as a more homogeneous cellular distribution along the PRF clot, as well as a greater accumulation and release of growth factors, in the protocols of reduced speed and time and in horizontal centrifugation compared to the standard protocol of L-PRF.[1,14,24–30]

However, the literature still needs to be more comprehensive regarding *in vivo* studies comparing the biological potential of PRF membranes produced by different protocols.[31–37] Thus, the present study aimed to evaluate bone neoformation in critical size defects (CSDs) treated with PRF membranes produced by fixed-angle and horizontal centrifugation protocols.

Methods

Animals

Thirty-two rats (*Rattus Norvergicus, Albinus*, Wistar), aged 14 weeks, with body mass between 350 g and 450 g, were obtained after submission and approval by the Committee on Ethics in the Use of Animals (CEUA) of the School of Dentistry of Ribeirão Preto (FORP) of Universidade de São Paulo (USP), under number 2019.1.930.58.0. The animals were kept in an environment with a 12-hour light cycle per day and a temperature between 22 and 24°C and consumed selected solid chow and water *ad libitum*.

The animals were randomly divided into four experimental groups (*n* = 8): Control (C), L-PRF, A-PRF, and H-PRF (Figure 1). The sample size ensured a power of 80% in the statistical analysis of the data obtained in the study, considering the means and standard deviations of the Area of Neoformed Bone (ANB) in the experimental groups of previous studies,[38–40] adjusting the α value at 0.05.

The experimental surgical procedures (blood collection for preparing PRF and creating the defect) were performed after inhalation anesthesia of the animals in a chamber containing 4% isoflurane (Instituto Biochimico Ind. Farm. Ltda, Itatiaia, RJ, Brazil). In addition, the animals were given Morphine Sulfate 8 mg/Kg (Dimorf, Cristália ® Prod. Quím. Farm. Ltda, Itapira, SP, Brazil) intramuscularly; Flunixin Meglumine 2 mg/Kg (Aplonal 1%, König ®, Buenos Aires, Argentina) subcutaneously; and 24 000 IU/Kg of penicillin G-benzathine (Pentabiotic Veterinário Pequeno Porte, Fort Dodge Animal Health ®, Campinas, SP, Brazil) intramuscularly.
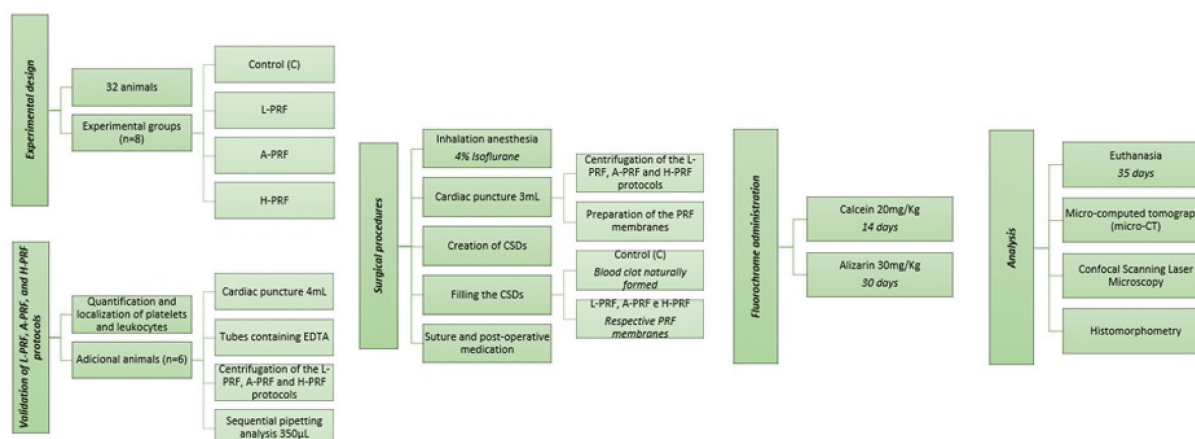

Figure 1. Flowchart of the study design.

Blood collection and PRF processing

Three milliliters of blood was obtained from each animal via cardiac puncture for the preparation of platelet-rich fibrin (PRF). Blood was collected in a 5 mL disposable syringe (Descarpack, São Paulo, Brazil) and stored in 5 mL silica-coated plastic tubes (BD Vacutainer®, Becton, Dickinson and Company, Franklin Lakes, NJ, USA) without the presence of anticoagulant substances, and immediately processed.

The cardiac puncture technique was employed to get a sufficient blood sample in a timely manner for the production of PRF membranes, being possible to obtain 3 mL of blood from each animal, according to the average body mass of the animals employed in this study, without causing suffering or extrapolate physiological limits.[41,42]

PRF collection followed three different protocols. In the L-PRF group, blood was centrifuged at a speed of 2700 revolutions per minute (rpm) for 12 minutes (~700 g maximum Relative Centrifugal Force [RCFmax], corresponding to the maximum force applied to the tubes and calculated at the bottom of the centrifugation[43] in an Intra-Spin™ centrifuge (33° of rotor angle, 55 mm of rotor radius at the height of the clot, 86 mm of maximum radius; Intra-Lock® International, Inc, Boca Raton, FL, USA). In the A-PRF group, blood was centrifuged at 1500 rpm for 14 minutes (~200 g RCFmax,[28] also in an Intra-Spin™ centrifuge. Finally, a horizontal centrifuge (Eppendorf 5702 centrifuge, Hamburg, Germany) was used in the H-PRF group. Blood was centrifuged at an RCFmax of 700 g for 8 minutes (~2000 rpm), according to a protocol previously established in the literature.[14]

After processing, the intermediate portion, representing the PRF clot, was collected and processed to fill the defects in the calvaria of animals in the L-PRF, A-PRF, and H-PRF groups.

Validation of L-PRF, A-PRF, and H-PRF protocols

To quantify and determine the location of cells along the tube after centrifugation and production of PRF, sequential pipetting analysis was performed using an adaptation of the work by Miron et al.[9] Six rats (two for each PRF protocol) were subjected to the collection of 4 mL of blood in tubes containing EDTA, so that, after centrifugation, the layers were separated. Still, no clot was formed, allowing the layers to be pipetted to laboratory analyses. After centrifugation of the L-PRF, A-PRF, and H-PRF protocols, 350-μL layers were pipetted sequentially, from the most superficial layer to the bottom of the tube, totaling ten samples per tube. These samples were stored in Eppendorf flasks and sent for quantification of platelets, leukocytes, and red blood cells to verify the location of these cells along the tube.

Creation of CSD

After blood collection for PRF preparation, a 5-mm diameter CSD was created on the calvaria of each animal using a trephine bur (5-mm Trephine Burr, Neodent®, Curitiba, PR, Brazil) at low rotation under constant irrigation with sterile saline solution. Defects from group C were filled with blood clots, naturally formed after the creation of CSDs. Defects from groups L-PRF, A-PRF, and H-PRF were filled with respective PRF membranes. The PRF membranes were divided approximately in half with the aid of surgical scissors. The portion closest to the red cells was cut into small pieces and used to fill the defect. The other half of the membrane was used to cover the defect in order to keep the material inside.

Tissues were joined in single sutures with 4.0 silk thread (Ethicon®, Johnson & Johnson, São José dos Campos, SP, Brazil) to achieve primary wound closure. Postoperatively, each

animal received an injection of tramadol hydrochloride at 20 mg/kg (Cronidor 2%, Agener União®, Apucarana, PR, Brazil) and flunixin meglumine at 2 mg/kg (Aplonal 1%, Könir®, Buenos Aires, Argentina) every 12 hours for two days.

Fluorochrome administration

At 14 days after making the CSDs, the animals received fluorochrome calcein (20 mg/Kg) intramuscularly. At 30 days after making the CSDs, alizarin red fluorochrome (30 mg/kg) was also administered intramuscularly. The administration of calcein allows the visualization of calcium deposition in the old bone, while alizarin enables its observation in the newly formed bone.[44–46]

Euthanasia

The animals were euthanized 35 days after the making of the CSDs, using a CO2 chamber with controlled flow after anesthesia with the association of 10% Ketamine (80 mg/Kg) and 2% Xylazine (10 mg/Kg). Samples of the calvaria containing the area of the original surgical defect and the surrounding tissues were removed *en bloc* with a diamond disc and fixed in a 10% neutral buffered formalin solution for 24 hours. Then, they were washed in running water for another 24 hours and identified and stored in flasks containing 70° alcohol.

Analysis by micro-computed tomography (micro-CT)

Undecalcified samples of the calvaria were scanned by a SkyScan 1172 cone-bean micro-CT (SkyScan N.V., Kontich, Belgium) to generate three-dimensional (3D) images. Using DataViewer software v. 1.4.3 (SkyScan N.V., Kontich, Belgium), the 3D image was rotated to a standard position for analysis. Then a 5-mm diameter region of interest (ROI) and a volume of interest (VOI) of $0.5 \times 5 \times 5$ mm was determined. To evaluate the trabecular bone tissue present in the calvaria in each VOI, a grayscale (0–255) was used, adopting the threshold between 80 (minimum) and 170 (maximum).

Using the CT-Analyzer® v.1.13.5.1+ software (Bruker, Kontich, Belgium), the following structural parameters were evaluated in each VOI by a calibrated examiner (L.M.S.P): i) BV – the percentage of VOI filled by bone tissue; ii) BP – the percentage of porosity present in the bone tissue determined in the VOI; iii) Tb. N – number (mm^{-1} of bone trabeculae present in the VOI; iv) Tb.Sp – total spaces (mm) between the bone trabeculae in the VOI; v) Conn.Dn – connectivity density between the bone trabeculae present in the VOI.

Confocal scanning laser microscopy

Laboratory processing

The dynamics of bone neoformation were evaluated by means of fluorescence analysis, according to previously published protocols.[44–46]

The pieces obtained were fixed in a 10% formalin solution with pH 7 for 10 days, with the solution being changed every two days. After this period, the pieces were transferred to recipients containing increasing solutions of alcohol for dehydration (70%, 80%, 96%, and 100%), being subjected to agitation at each change. The samples were placed in polyethylene containers containing pure resin (LR White Hard Grade, London, UK) and under agitation for 60 minutes. After this period, the pieces were stored and kept in a refrigerator at 4°C for at least 12 hours. Then, the pieces were kept in a vacuum for one hour, shaken for the same period, and again stored in a refrigerator at 4°C for 24 hours. This routine was repeated for 15 days, changing the resin every

48 hours. On the 15th day, after changing the resin, the pieces were placed in Teflon molds and taken to the oven at 60°C for 12 hours for the resin polymerization. The polymerized resin blocks containing the samples were then cut in half using an Exakt system, using a diamond saw, and continuous irrigation with water. The surfaces containing the samples were ground in the Exakt system using sandpaper with increasing grit (320, 800, 2500, 4000) until the part's surface was smooth. The sanded and polished blocks were then glued to an acrylic sheet using the Exakt system, and the exposed surface of the piece glued to the sheet was sanded and polished again until a thickness of approximately 70 μm was obtained.

Image analysis

The pieces were scanned with a Trinocular Motorized Microscope for Immunofluorescence and Bright Field (model AXIO IMAGER M2, Carl Zeiss®, Germany) with a 10× objective coupled to an AxioCam MRm Rev.3 FireWire camera (Carl Zeiss®). After image reconstruction using AxioVision Rel. 4.8 (Carl Zeiss®, Germany), it was possible to visualize the calcein precipitation at 14 days (Figure 2a), evidenced by the green color, representing the deposition of calcium in the old bone, and the precipitation of alizarin at 30 days (Figure 2b), in red color, which demonstrates the deposition of calcium in the newly formed bone. The overlapping of the two layers of fluorochromes was performed, allowing the visualization of calcium deposition in both periods, which represents the conversion of old bone into newly formed bone (Figure 2c). The images were standardized in hue, saturation, and brightness. Image captures were performed in the center of the CSD and the regions close to the original borders of the defect.

The saved images were then transferred to the Image J program (Processing Software and Image Analysis, Ontario, Canada). For each analyzed sample, calcein was delimited in a central region of the CSD with the "freehand" tool, measuring the area in mm[2]; the same procedure was performed with alizarin. Calcein and alizarin values allow the observation of the dynamics of bone neoformation and its comparison between different experimental groups.[44–46]

Histomorphometric analysis

After performing Confocal Microscopy, the slides already processed were stained with Stevenel Blue and Alizarin Red for analysis with light microscopy. In each section, the histopathological characteristics of the newly formed bone tissue were analyzed.

Histometric analysis was performed by a blinded and calibrated examiner (D.S.F.S.) using a computer image assessment system and image acquisition and analysis software (LAS EZ version 4.1.0, Leica Mycrosystems®). One histological section of the central area of the surgical defect of each specimen was

selected (in each experimental group, eight images were analyzed). Each histological section was photographed using a trinocular microscope for brightfield and fluorescence (DMLB, Leica Mycrosystems® Wetzlar GmbH, Heidelberg, Germany) with a 1.6× objective coupled to a DFC300FX camera (Leica Mycrosystems®). In each image, a delimitation of the analyzed area was performed, corresponding to the region of the calvaria bone where the defect was created, called Total Area (TA). Within the TA, the Area of Neoformed Bone (ANB) was selected and delimited. The TA value was considered 100% of the analyzed area, and the ANB value was calculated as a percentage of TA.

The histopathological analysis was performed by observing the same selected histological sections using the same microscope, with 10× and 20× objectives coupled to the same camera used in the histometric analysis.

Statistical analysis

Analyzes were performed using GraphPad Prism software (GraphPad Software, Inc, v. 5.01, San Diego, CA, USA). The animal was considered as the statistical unit. A significance level of 5% was chosen ($p < .05$). Data distribution was verified by the Shapiro-Wilk test. The significance of differences between groups for all variables was determined by analysis of variance (ANOVA), followed by Tukey's post-hoc test.

Results

Validation of platelet concentrates protocols

The quantification and location of platelets and leukocytes throughout the tube after centrifugation and production of PRF by three protocols (L-PRF, A-PRF, and H-PRF) were investigated by means of sequential pipetting analysis and represented in Table I.

It was observed that in the L-PRF protocol, platelets and leukocytes were significantly concentrated in layer 5, in the region of the interface between the portion corresponding to the PRF and the red cell layer, corresponding to 62.6% and 40.2% of the total of these cells after centrifugation, respectively. It was not possible to observe the presence of leukocytes in the first 4 layers of the tube. A large number of leukocytes was also found in the red cell layer below the region corresponding to the PRF.

In turn, in the A-PRF protocol, there was a higher concentration of platelets and leukocytes in layers 4 and 5, totaling ~ 55% and almost 40% of the total of these cells after centrifugation, respectively. Compared to the L-PRF, platelets, and leukocytes were more homogeneous and distributed throughout the tube. However, leukocytes were also not observed in the first two layers.

In the H-PRF protocol, it was possible to observe a high concentration of platelets in the first 4 layers of the tube, evenly distributed in these layers, corresponding to 87.4% of the total of
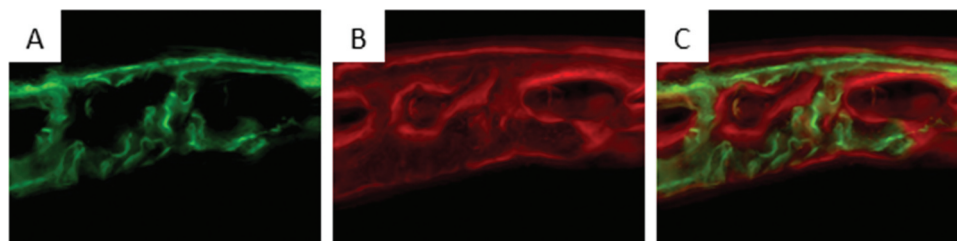

Figure 2. Images of the center of the CSD obtained by confocal microscopy. (a) Calcein precipitation (green); (b) Alizarin precipitation (red); (c) Overlap of images, showing both fluorochromes.

Table I. Percentual distribution of platelets and leukocytes in all layers (A1-A10) after blood centrifugation to prepare L-PRF, A-PRF and H-PRF.

layers	platelets (%)			leukocytes (%)		
	L-PRF	A-PRF	H-PRF	L-PRF	A-PRF	H-PRF
A1	0.55	5.15	16.08	0	0	0
A2	1.58	4.36	28.66	0	0	13.90
A3	0.57	6.71	25.75	0	5.59	13.79
A4	0.45	29.30	16.89	0	13.49	23.17
A5	62.58	25.69	2.81	40.16	26.31	16.59
A6	16.27	5.75	3.54	12.94	7.90	13.25
A7	4.44	5.32	1.64	12.56	14.09	8.84
A8	1.38	5.24	1.19	2.24	18.10	3.77
A9	3.90	4.41	1.61	12.94	5.53	4.52
A10	8.27	8.06	1.82	19.15	8.99	2.15

these cells in the tube after centrifugation. A more homogeneous distribution of leukocytes was also found between layers 2 and 6, representing 80.7% of the total leukocytes after centrifugation.

Analysis by micro-computed tomography (micro-CT)

The three-dimensional reconstructions were obtained from the calvaria and the means and standard deviations of BV, BP, Tb. N, Tb.Sp, and Conn.Dn for all experimental groups are shown in Figure 3. The H-PRF group ($n = 8$) showed higher statistically significant values ($p < .05$) of BV (11.83 ± 7.399) and Tb. N (0.8929 ± 0.5553) when compared to groups C ($n = 8$; BV: 2.096 ± 1.749; Tb. N: 0.3426 ± 0.3151), L-PRF ($n = 8$; BV: $4.96 \pm 1,807$; Tb. N: 0.3431 ± 0.1744), and A-PRF ($n = 8$; BV: 5.733 ± 2.399; Tb. N: 0.4358 ± 0.1571). In the analysis of BV, L-PRF, and A-PRF showed significantly higher values ($p < .05$ and $p < .01$, respectively) than those of group C, with no significant differences between groups L-PRF and A-PRF for this parameter ($p > .05$). In the analysis of Tb.N, no statistically significant differences were found among groups C, L-PRF, and A-PRF ($p > .05$). For the microtomographic parameters of BP and Tb.Sp, no statistically significant differences ($p > .05$) were found among groups C (BP: 95.71 ± 4.497; Tb.Sp: 0.5085 ± 0.02597), L-PRF (BP: $95.48 \pm 2,081$; Tb.Sp: 0.5134 ± 0.009539), A-PRF (BP: $94.27 \pm 2,399$; Tb.Sp: 0.5006 ± 0.1521) and H-PRF (BP: $90.75 \pm 7,892$; Tb.Sp: 0.4896 ± 0.04201). In the Conn.Dn analysis, statistically significant differences ($p < .05$) were observed only between the H-PRF (35.14 ± 18.63) and A-PRF (18.13 ± 8.227) groups. Groups C (18.56 ± 10.86) and L-PRF ($16.5 \pm 7,397$) did not present statistically significant differences between themselves or in relation to the other groups for the Conn.Dn parameter ($p > .05$).

Confocal scanning laser microscopy

Images obtained by Confocal Microscopy allowed the observation of bands of calcein (injected 14 days after creating the CSDs, green color) and alizarin (injected 30 days after making the CSDs, red color), formed by the precipitation of calcium in the organic matrix (Figure 4). In group C, in the central region (Figure 4a), small markings of calcein and alizarin were observed, which were superimposed, with a thickness much smaller than that found in the region close to the margins of the original defect. In the area close to one of the original borders (Figure 4b), a thin layer of calcein and alizarin was observed, demonstrating the slow process of bone neoformation. In the L-PRF and A-PRF groups, greater precipitation of calcein and alizarin was observed in the central region (Figure 4c,e) and in the region close to one of the original borders (Figure 4d,f), manifested by the greater intensity in fluorescence. In the H-PRF group, the central region (Figure 4g) showed intense labeling of calcein and alizarin, evidencing a higher rate of bone neoformation and lower rates of resorption of old bone. In addition, the thickness observed in the central region of the defect was very close to that present in the region close to the margins of the original defect. In the region close to one of the original borders (Figure 4h), more evident bands of calcein and alizarin were also observed compared to group C.

Figure 5 represents the means and standard deviations of calcein and alizarin for all experimental groups. Intragroup analysis showed statistically significant differences between fluorochromes injected at 14 days (calcein) and 30 days (alizarin) ($p < .05$), manifested by higher alizarin labeling and lower calcein labeling in the L-PRF groups ($n = 8$; CA: 0.0516 ± 0.02406; AL: 0.0865 ± 0.04706) and H-PRF ($n = 8$; CA: 0.0684 ± 0.06011; AL: 0.1283 ± 0.01332), indicating an increased bone turnover (Figure 5a). In groups C ($n = 8$; CA: 0.02375 ± 0.01575; AL: 0.0268 ± 0.01230) and A-PRF ($n = 8$; CA: 0.0704 ± 0.03750; AL: 0.0756 ± 0.04430), no statistically significant differences were observed between the area stained by calcein and the area stained by alizarin, indicating a slower bone neoformation process.

Higher statistically significant values of calcein were found in the L-PRF, A-PRF, and H-PRF groups compared to the C group (Figure 5b). No statistically significant differences were found between the L-PRF, A-PRF, and H-PRF groups regarding calcein precipitation. The H-PRF group showed the highest alizarin labeling, with statistically significant differences in relation to the C, L-PRF, and A-PRF groups (Figure 5c). The L-PRF and A-PRF groups had statistically significant higher values of alizarin in relation to the C group. There were no statistically significant differences in alizarin between the L-PRF and A-PRF groups.

Histomorphometric analysis

Histometric analysis

The means and standard deviations of ANB and the result of the intergroup comparisons are represented in Figure 6. The H-PRF group ($n = 8$; ANB = 12.67 ± 9.247) showed the highest statistically significant values of ANB ($p < .01$; $p < .05$ and $p < .01$, respectively) compared to groups C ($n = 8$; 0.2125 ± 0.3934), L-PRF ($n = 8$; 3.682 ± 3.176) and A-PRF ($n = 8$; 2.129 ± 1.783). The L-PRF and A-PRF groups showed higher ANB values than the C group ($p < .01$ and $p < .05$, respectively). No statistically significant differences in ANB were found for the L-PRF and A-PRF groups ($p > .05$).

Histopathological analysis

Control group. A connective tissue composed of collagen fibers oriented parallel to the wound's surface was observed along almost the entire length of the surgical defect. In the central part of the defect there was a thickness much smaller than that found in the original bone tissue of the cap. Along the margins of the surgical defect, a small amount of newly formed bone tissue was observed, showing a small number of osteoblasts on its edges (Figure 7a,b). In all specimens, a small number of blood vessels and a moderate number of fibroblasts were found. A generally mild inflammatory infiltrate was also observed, with lymphocytes and plasma cells, distributed along the defect.
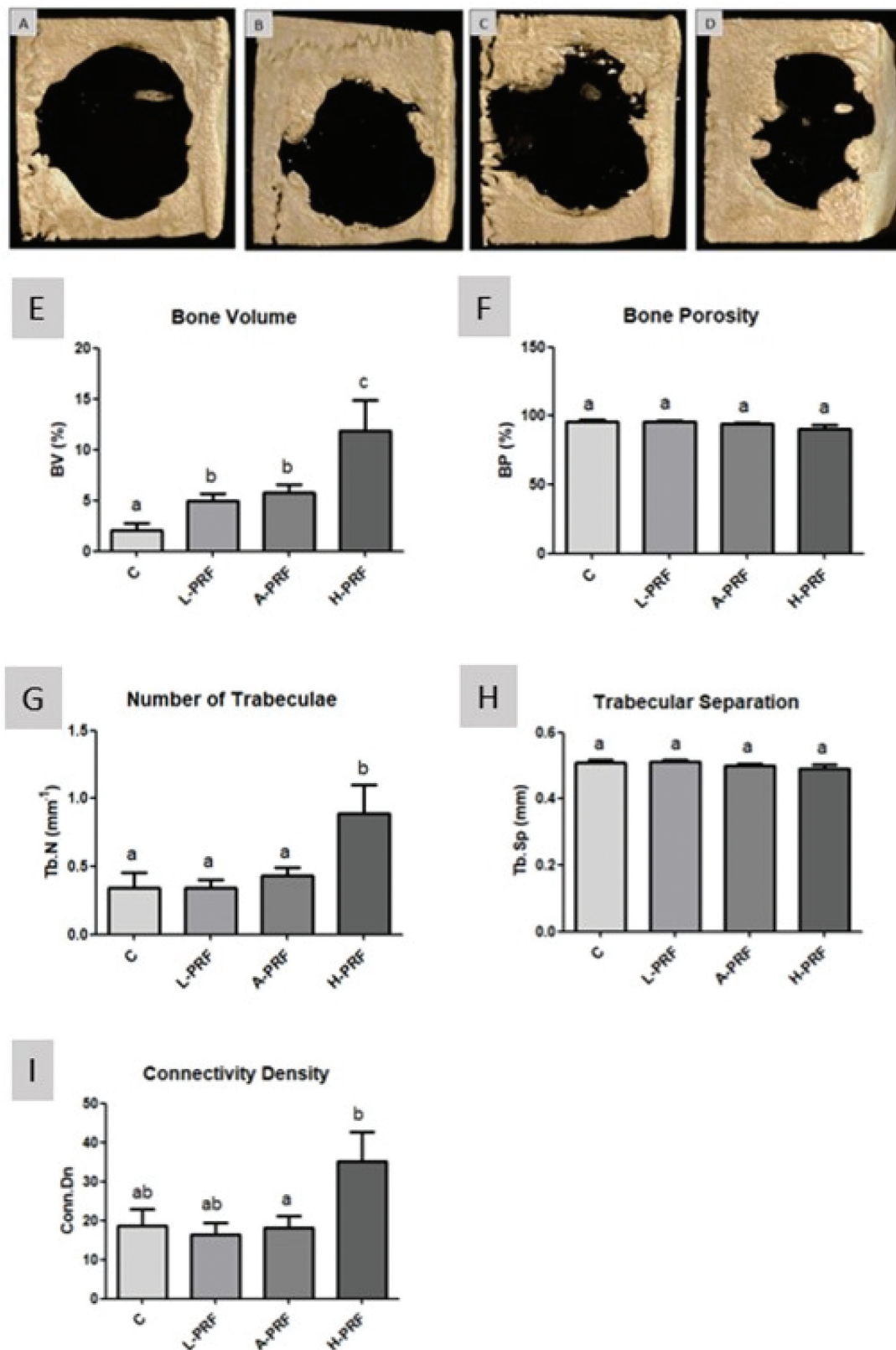
Figure 3. Micro-CT of the calvaria. Rendered reconstructions of the Control (a), L-PRF (b), A-PRF (c), and H-PRF (d) groups calvaria. Pixel size = 15.9 μm. Means and standard deviations (SD) of BV (e), BP (f), Tb.N (g), Tb.Sp (h) and Conn.Dn (i) of groups C, L-PRF, A-PRF and H-PRF, with the results of comparisons between groups. Different letters indicate statistically significant differences ($p < .05$).

L-PRF group. The newly formed bone tissue exhibited a small number of osteoblasts at its edges. The connective tissue presented numerous bundles of collagen fibers arranged parallel to the wound surface, but more organized and thicker than those observed in specimens from Group C, although still smaller than the thickness of the surgical defect margin. Most specimens from the L-PRF Group had a greater amount of newly formed bone tissue near the margins of the surgical defect when compared to specimens from Group C (Figure 7c,d). In some specimens, bone neoformation was

Figure 4. Images obtained by confocal microscopy showing the overlapping of calcein (green) and alizarin (red) in the experimental groups. Representative images of the center of the CSD (a, c, e, g) and the region close to margins of the original surgical defect (b, d, f, h). Groups: C (A, B); L-PRF (c,d); A-PRF (E,F); H-PRF (g,h). Arrows represent the margins of the original surgical defect. Original magnification = 10×.

also observed along the defect, forming islets. In addition, a significant presence of blood vessels was observed along its entire length.

A-PRF group. The newly formed bone tissue exhibited a small number of osteoblasts at its edges. The connective tissue had numerous bundles of collagen fibers arranged
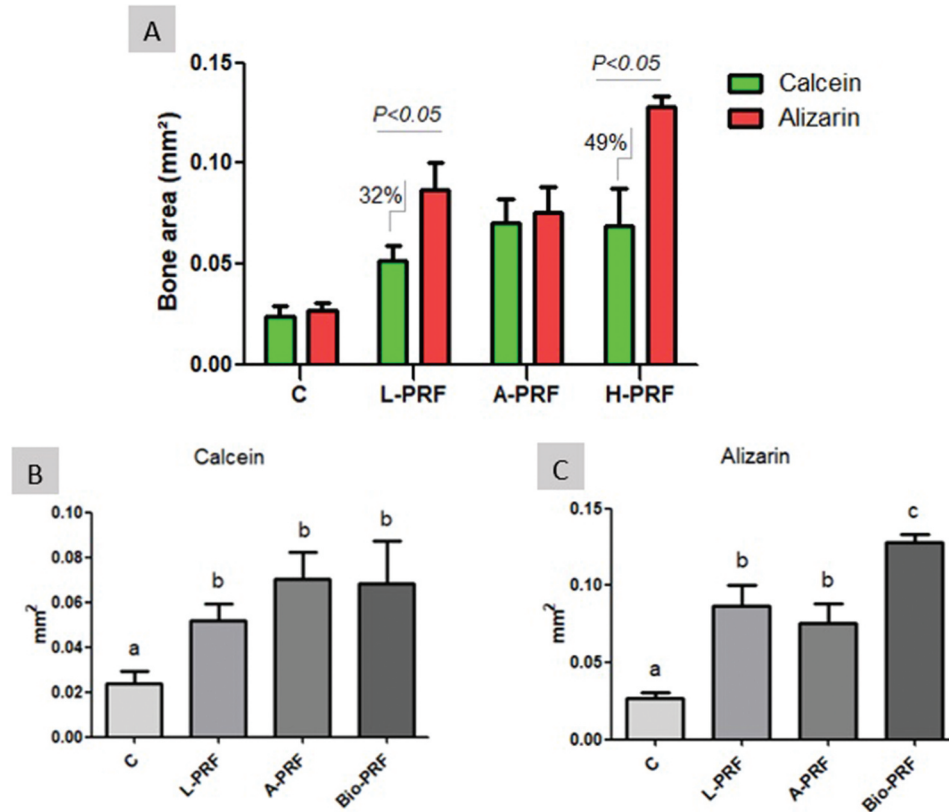
Figure 5. Means and standard deviations for calcein and alizarin precipitations for groups C, L-PRF, A-PRF and H-PRF, with the results of intragroup and intergroup comparisons. * indicates statistically significant differences ($p < .05$).

Figure 6. Means and standard deviations for ANB for groups C, L-PRF, A-PRF and H-PRF, with the results of comparisons between groups. Different letters indicate statistically significant differences ($p < .05$).

parallel to the wound surface but were more organized and thicker than those observed in specimens from Group C. Most samples from the A-PRF Group had a more significant amount of newly formed bone tissue along the margins of the surgical defect when compared to specimens

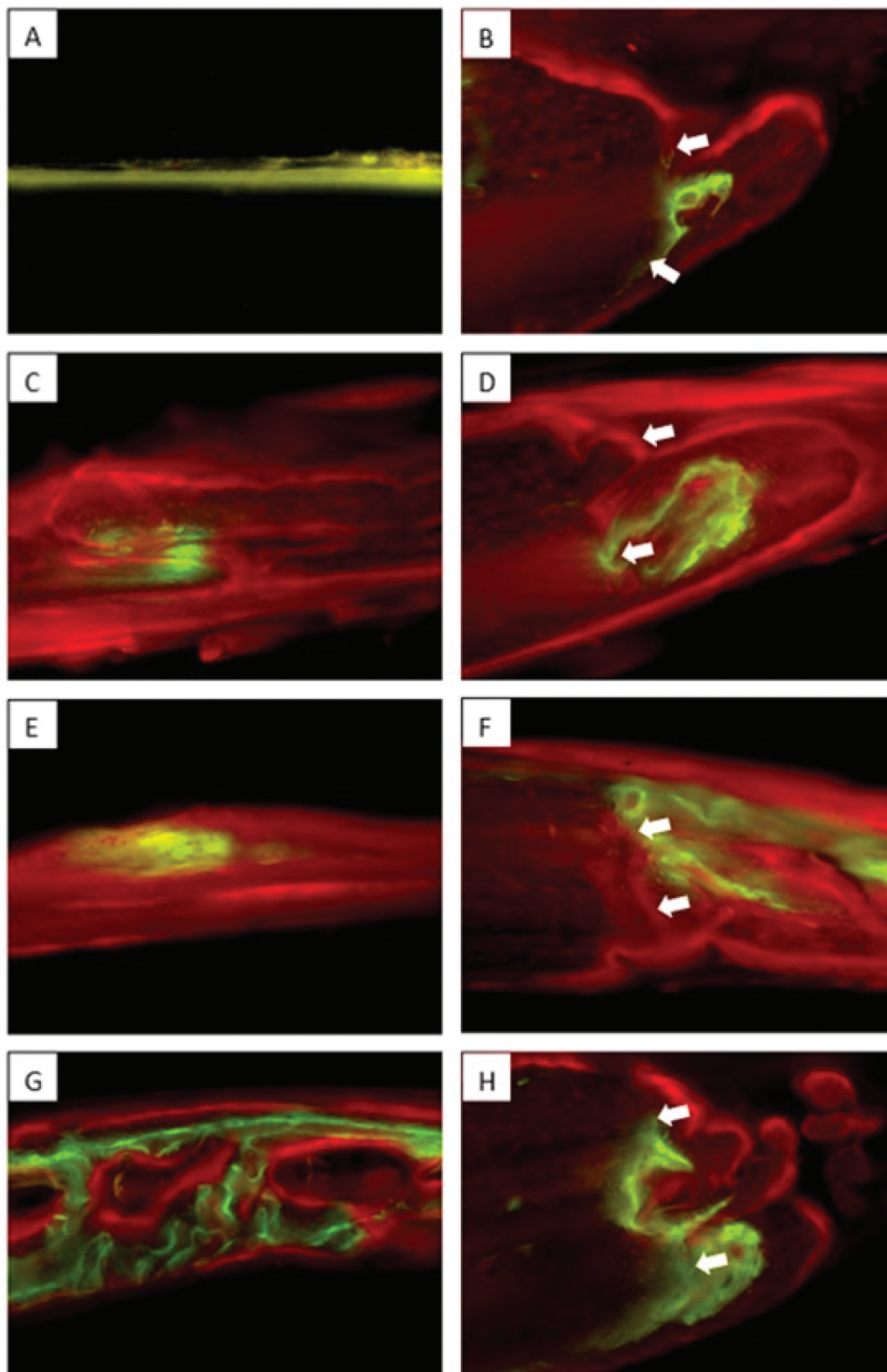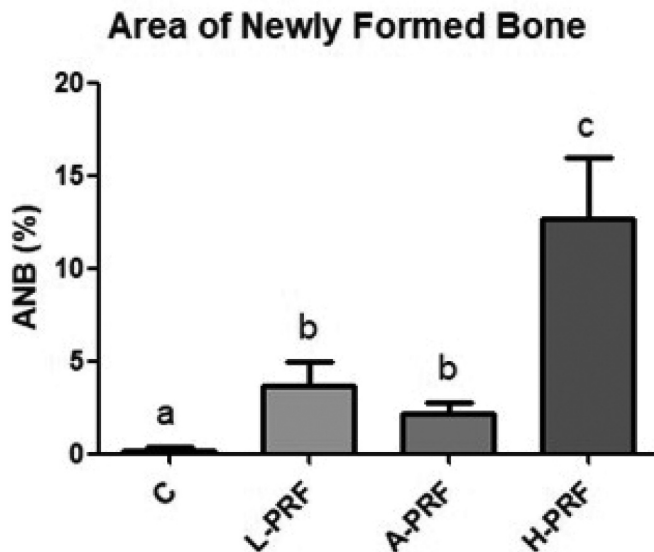from Group C (Figure 7e,f). In some specimens, bone neoformation was also observed along the defect, forming islets. In addition, a significant presence of blood vessels was observed along its entire length.

H-PRF group. The newly formed bone tissue exhibited numerous osteoblasts at its edges. The connective tissue had numerous bundles of collagen fibers arranged parallel to the wound surface but were more organized and thicker than those observed in specimens from Group C. Most specimens from the H-PRF Group had a greater amount of newly formed bone tissue along the margins of the surgical defect when compared to specimens from Group C, L-PRF, and A-PRF. In most specimens, intense bone neoformation was also observed along the defect, forming islets (Figure 7g,h). In addition, a significant presence of blood vessels was observed along its entire length.

Discussion

In recent years, literature has focused on proposing new formulations of platelet concentrates obtained by centrifugation of autologous blood, with the objective of improving the structural and molecular characteristics of these matrices, such as mechanical strength and retention and release rates of growth factors. Variations in Relative Centrifugal Force (RCF) and centrifugation time, as well as the introduction of new centrifuges and tubes for blood collection, led to changes in the original method proposed by Choukroun et al.[7] and the emergence of new protocols such as
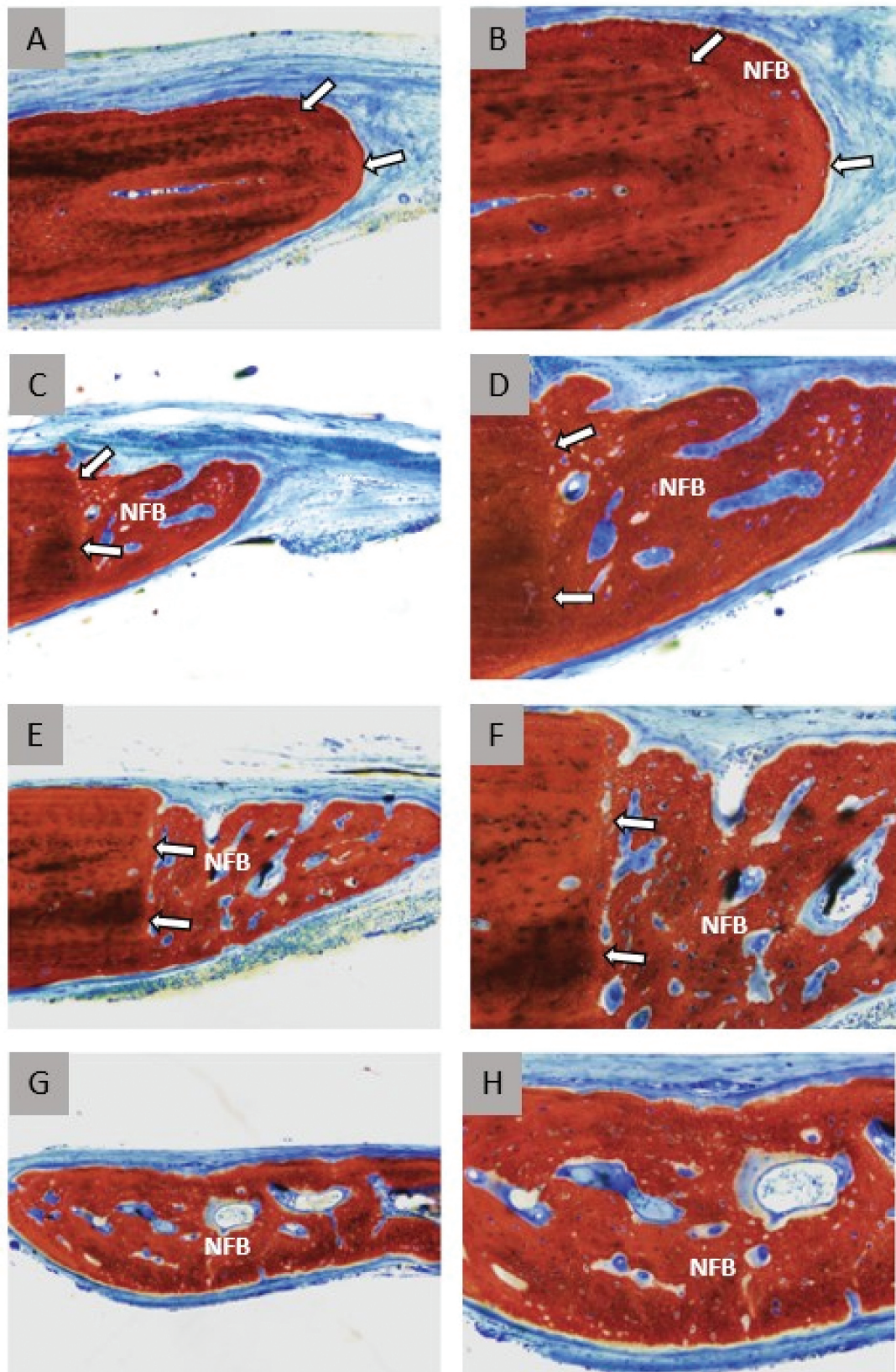
Figure 7. Representative images of histological sections. Groups: C (a, b); L-PRF (c, d); A-PRF (e, f); H-PRF (g, h). NFB = newly formed bone; unfilled arrow = margins of the original surgical defect. *Images G, H represent portions distant from the margins of the original surgical defect. Coloration: Stevenell Blue and Alizarin Red. Original magnification = 10× (a, c, e, g); 20× (b, d, f, h).

A-PRF, and PRF obtained by horizontal centrifugation (H-PRF).[27] However, the biological impact in *in vivo* studies of these modifications is still an obscure field in the literature. The present study is the first to evaluate bone neoformation in CSDs created in rat calvaria and treated with platelet concentrates of autogenous origin, obtained by three different protocols involving

high and low-speed centrifugation as horizontal and fixed-angle centrifugation equipment. The results obtained showed, in short, that platelet concentrates potentiate bone neoformation in CSDs in rat calvaria. However, the horizontal centrifugation protocol produced platelet concentrates with greater biological potential for bone regeneration.

This study used three different centrifugation protocols to obtain PRF membranes. The PRF membranes produced with rat blood showed similar characteristics to the PRF produced with human blood in terms of cell number and distribution, according to findings from previous studies.[1,14,47] It is possible to observe that the protocols of low-speed centrifugation and protocols using horizontal centrifugation were more effective in concentrating platelets and distributing them more evenly along the PRF matrix than the original L-PRF protocol. Regarding leukocytes, horizontal centrifugation promoted a 2-fold increase in the number of cells, as well as a more uniform distribution between the PRF layers, when compared to fixed-angle centrifugation protocols.

Fluorescence analysis by confocal microscopy has been widely used in studies involving the evaluation of bone regeneration due to the ability of fluorochromes to bind to calcium ions at the time of their precipitation in the matrix, and the amount of fluorescence allows direct visualization of the amount of bone present. The administration of different fluorochromes in different periods allows the evaluation and differentiation of the old bone and the neoformed bone, which, in turn, enables the measurement of the phenomenon of bone neoformation.[44–46] This study observed increased bone turnover in the L-PRF and H-PRF groups, demonstrated by the higher alizarin labeling and lower calcein labeling. Furthermore, the greater presence of calcein in the L-PRF, A-PRF, and H-PRF groups compared to the control group indicates lower rates of bone resorption. In contrast, the more expressive presence of alizarin in the H-PRF group highlights its potential to promote neoformation bone. In general, all PRF matrices stimulated the process of bone neoformation in the present study. The cell concentration and release of growth factors make PRF an ideal biological framework, promoting the acceleration of cell migration and proliferation, angiogenesis, modulation of the immune response, and recruitment of undifferentiated mesenchymal cells, which favors the repair and regeneration of soft and hard tissues.[6,8–13]

Previous studies have already demonstrated the potential of L-PRF and A-PRF in accelerating bone neoformation of CSDs created in rat calvaria. Higher amounts of newly formed bone were demonstrated in microtomographic and histomorphometric analyses, in statistically significant values, compared to filling the CSDs with clot alone (control group).[37] Furthermore, the association of L-PRF with bovine xenograft promoted higher rates of neoformed bone in microtomographic and histomorphometric parameters against experimentally induced osteoporosis and greater expression of essential growth factors for the promotion of bone regeneration, compared to the control group.[48]

The present study produced PRF matrices using high and low-speed centrifugation. *In vitro*, studies have demonstrated better cellular and molecular characteristics in low-speed centrifugation protocols.[1,28,49,50] It is thus assumed that structural changes in PRF clots may alter their regenerative potential. In all parameters analyzed in this study, no statistically significant differences were found between the L-PRF and A-PRF groups, which supports the findings of Silva et al. (2022),[37] where the two different types of PRF matrices promoted greater bone neoformation compared to the control group, in microtomograhpic and histomorphometric parameters, but there were no significant differences between them. Higher rates of release of important growth factors for the promotion of bone neoformation have been demonstrated in low-speed centrifugation protocols compared to the original high-speed centrifugation protocols.[24,28]

On the other hand, Dohan Ehrenfest et al.[51] observed that the slow release of some growth factors from the original L-PRF membranes was significantly more potent at all experimental times than the release from the A-PRF membranes. It is important to emphasize that more critical than the number of platelets or growth factors present in the PRF samples is the dynamics in the interrelationship between platelets, leukocytes, fibrin, and growth factors.[28] It is not just the amount that matters, but how the cells/molecules are distributed in the PRF matrix, their retention level, and their release pattern.

In an unprecedented way, the present study evaluated with proper statistical power the biological impact of PRF matrices produced from different centrifugation angles on bone regeneration. Membranes produced by horizontal centrifugation provided higher values of BV, Tb. N, ANB, and higher expression of Alizarin, compared to those produced by centrifuges with fixed-angle rotors. In fact, over the years, new protocols have been proposed based on concepts of low speed and reduced time centrifugation, such as A-PRF and i-PRF, in addition to the introduction of horizontal centrifugation (H-PRF), to improve the structural characteristics of PRF membranes and increase the bioavailability of cells and growth factors, which could potentiate their regenerative effects.[1,14,24,25,28,47,52,53]

In the present study, H-PRF samples showed a more homogeneous distribution of leukocytes and a 7.7-fold increase compared to peripheral blood samples. This increase was also higher than those observed in the L-PRF and A-PRF samples. This information supports findings from previous studies, where horizontal centrifugation allowed a 4-fold increase in the number of cells (especially leukocytes) present in the layers corresponding to PRF compared to fixed-angle centrifugation.[14] White blood cells, in particular, are important during wound healing, especially during biomaterial integration and tissue formation.[54–59]

In summary, the present study demonstrated that using fixed-angle centrifuges, the centrifugation speed in the production of platelet concentrates did not alter their biological potential. Both L-PRF and A-PRF promoted comparable results in hard tissue regeneration. However, H-PRF increased BV by 464%, 238%, and 206% in relation to control, L-PRF, and A-PRF groups. The differences between H-PRF and other platelet concentrates reported in several *in vitro* studies[14,26,47,57] may explain these results. It is important to highlight that the literature is still controversial regarding predictability in PRF treatment, especially in bone regeneration. High-quality randomized controlled clinical studies and meta-analyses are required to reverse this limitation of the literature. Therefore, it is essential to standardize the protocols for preparing and applying PRF matrices, minimizing the occurrence of variables that can compromise the effectiveness, treatment, and final result.[30,51]

Data from this study should be interpreted with caution. The preparation of autologous platelet concentrates in rats required adaptations of the original protocols regarding the total volume of blood collected in each tube. A recent publication has standardized the PRF preparation process for animal studies, emphasizing the importance of a consistent method for evaluating these platelet concentrates.[60] This standardization is crucial for ensuring the reliability and comparability of results in animal-based PRF research. Although the present study did not focus on measuring growth factor levels in PRF samples, addressing this aspect in future investigations is necessary to understand the potential impact on experimental outcomes better. Furthermore, isolated PRF matrices were used in the creation of CSDs. Future studies evaluating the association of these matrices with biomaterials, as well as evaluating the correlation between the levels of growth factors, number of platelets, and amount of newly formed bone, are important. Longer follow-up periods, in addition to the use of

animals with systemic compromises and animals with a larger phylogenetic scale, should also be performed to elucidate better the role of platelet concentrates in promoting tissue neoformation.[37]

Conclusion

Within the limits of this study, it can be concluded that: i) the platelet concentrates L-PRF, A-PRF, and H-PRF potentiate bone neoformation in CSDs in rat calvaria; ii) the horizontal centrifugation protocol produces a PRF with greater biological potential for bone regeneration.

Disclosure statement

No potential conflict of interest was reported by the author(s).

Funding

ORCID

Débora de Souza Ferreira Sávio ⓘ http://orcid.org/0000-0003-4073-0297
Lucia Moitrel Pequeno da Silva ⓘ http://orcid.org/0000-0003-3317-8393
Gabriel Guerra David Reis ⓘ http://orcid.org/0000-0002-9541-5238
Ricardo Junior Denardi ⓘ http://orcid.org/0000-0001-8312-7493
Natacha Malu Miranda da Costa ⓘ http://orcid.org/0000-0001-7852-4697
Flávia Aparecida Chaves Furlaneto ⓘ http://orcid.org/0000-0002-8072-3983
Sérgio Luís Scombatti de Souza ⓘ http://orcid.org/0000-0002-6199-7348
Carlos Fernando de Almeida Barros Mourão ⓘ http://orcid.org/0000-0001-5775-0222
Richard J. Miron ⓘ http://orcid.org/0000-0003-3290-3418
Roberta Okamoto ⓘ http://orcid.org/0000-0002-6773-6966
Michel Reis Messora ⓘ http://orcid.org/0000-0001-8485-9645

References

1. Ghanaati S, Booms P, Orlowska A, Kubesch A, Lorenz J, Rutkowski J, Landes C, Sader R, Kirkpatrick C, Choukroun J. Advanced platelet-rich fibrin: a new concept for cell-based tissue engineering by means of inflammatory cells. J Oral Implantol. 2014;40(6):679–89. doi:10.1563/aaid-joi-D-14-00138.

2. Miron RJ, Zuchelli G, Pikos MA, Salama M, Lee S, Guillemette V, Fujioka-Kobaiashi M, Bishara M, Zhang Y, Wang H-L, et al. Use of platelet-rich fibrin in regenerative dentistry: a systematic rewiew. Clin Oral Invest. 2017;21(6):1913–27. doi:10.1007/s00784-017-2133-z.

3. Dohan DM, Choukroun J, Diss A, Dohan SL, Dohan AJ, Mouhyi J, Gogly B. Platelet-rich fibrin (PRF): a second-generation platelet concentrate. Part I: technological concepts and evolution. Oral Surg Oral Med Oral Pathol Oral Radiol Endod. 2006;101 (3):37–44. doi:10.1016/j.tripleo.2005.07.008.

4. Dohan Ehrenfest DM, Rasmusson L, Albrektson T. Classification of platelet concentrates: from pure platelet-rich plasma (P-PRP) to leucocyte- and platelet-rich fibrin (L-PRF). Trends Biotechnol. 2009;27(3):158–67. doi:10.1016/j.tibtech.2008.11.009.

5. Fijnheer R, Pietersz RN, De Korte D, Gouwerok CW, Dekker WJ, Reesink HW, Roos D. Platelet activation during preparation of platelet concentrates: a comparison of the platelet-rich plasma and the buffy coat methods. Transfusion. 1990;30:634–8. doi:10.1046/j.1537-2995.1990.30790385523.x.

6. Ghanaati S, Herrera-Vizcaino C, Al-Maawi S, Lorenz J, Miron RJ, Nelson K, Schwarz F, Choukroun J, Sader R. Fifteen years of

7. Choukroun J, Adda F, Schoeffler C, Vervelle A. Une opportunité en paro-implantologie: le PRF. Implantodontie. 2001;42:55–62.

8. Baslarli O, Tumer C, Ugur O, Vatankulu B. Evaluation of osteoblastic activity in extraction sockets treated with platelet-rich fibrin. Med Oral Patol Oral Cir Bucal. 2015;20(1):111–16. doi:10.4317/medoral.19999.

9. Choukroun J, Diss A, Simonpieri A, Girard MO, Schoeffler C, Dohan SL, Dohan AJ, Mouhyi J, Dohan DM. Platelet-rich fibrin (PRF): a second-generation platelet concentrate. Part IV: clinical effects on tissue healing. Oral Surg Oral Med Oral Pathol Oral Radiol Endod. 2006;101(3):56–60. doi:10.1016/j.tripleo.2005.07.011.

10. Dohan Ehrenfest DM, De Peppo GM, Doglioli P, Sammartino G. Slow release of growth factors and thrombospondin-1 in Choukroun's platelet-rich fibrin (PRF): a gold standard to achieve for all surgical platelet concentrates technologies. Growth Factors. 2009;27(1):63–9. doi:10.1080/08977190802636713.

11. Li Q, Reed DA, Min L, Gopinathan G, Li S, Dangaria SJ, Li L, Geng Y, Galang M-T, Gajendrareddy P, et al. Lyophilized platelet-rich fibrin (PRF) promotes craniofacial bone regeneration throught Runx2. Int J Mol Sci. 2014;15(5):8509–25. doi:10.3390/ijms15058509.

12. Soffer E, Ouhayoun JP, Anagnostou F. Fibrin sealants and platelet preparations in bone and periodontal healing. Oral Surg Oral Med Oral Pathol Oral Radiol Endod. 2003;95(5):521–8. doi:10.1067/moe.2003.152.

13. Zhao J-H, Tsai C-H, Chang Y-C. Clinical and histologic evaluations of healing in an extraction socket filled with platelet-rich fibrin. J Dent Sci. 2011;6:116–22. doi:10.1016/j.jds.2011.03.004.

14. Miron RJ, Chai J, Zheng S, Feng M, Sculean A, Zhang Y. A novel method for evaluating and quantifying cell types in platelet rich fibrin and an introduction to horizontal centrifugation. J Biomed Mater Res A. 2019;107(10):2257–71. doi:10.1002/jbm.a.36734.

15. Inchingolo F, Tatullo M, Marrelli M, Inchingolo AM, Scacco S, Inchingolo AD, Dipalma G, Vermesan D, Abbinante A, Cagiano R. Trial with platelet-rich fibrin and bio-oss used as grafting materials in the treatment of the severe maxillar bone atrophy: clinical and radiological evaluations. Eur Rev Med Pharmacol Sci. 2010;14 (12):1075–84. PMID: 21375140.

16. Temmerman A, Vandessel J, Castro A, Jacobs R, Teughels W, Pinto N, Quirynen M. The use of leucocyte and platelet rich fibrin (L-PRF) in socket management and ridge preservation: a split-mouth, randomised, controlled clinical trial. J Clin Periodontol. 2016;43(11):990–9. doi:10.1111/jcpe.12612.

17. Bajaj P, Pradeep AR, Agarwal E, Rao NS, Naik SB, Priyanka N, Kalra N. Comparative evaluation of autologous platelet rich fibrin and platelet-rich plasma in the treatment of mandibular degree II furcation defects: a randomized controlled clinical trial. J Periodontal Res. 2013;48(5):573–81. doi:10.1111/jre.12040.

18. Pradeep AR, Karvekar S, Nagpal K, Patnaik K, Raju A, Singh P. Rosuvastatin 1.2 mg in situ gel combined with 1: 1 mixture of autologous platelet-rich fibrin and porous hydroxyapatite bone graft in surgical treatment of mandibular class II furcation defects: a randomized clinical control trial. J Periodontol. 2016;87(1):5–13. doi:10.1902/jop.2015.150131.

19. Agarwal SK, Jhingran R, Bains VK, Srivastava R, Madan R, Rizvi I. Patient-centered evaluation of microsurgical management of gingival recession using coronally advanced flap with platelet-rich fibrin or amnion membrane: a comparative analysis. Eur J Dent. 2016;10(1):121–33. doi:10.4103/1305-7456.175686.

20. Keceli HG, Kamak G, Erdemir EO, Evginer MS, Dolgun A. The adjunctive effect of platelet-rich fibrin to connective tissue graft in the treatment of buccal recession defects: results of a randomized, parallel-group controlled trial. J Periodontol. 2015;86(11):1221–30. doi:10.1902/jop.2015.150015.

21. Tunali M, Ozdemir H, Arabaciota T, Gurbuzer B, Pikdoken L, Firatli E. Clinical evaluation of autologous platelet-rich fibrin in the treatment of multiple adjacent gingival recession defects: a 12-month study. Int J Periodontics Restorative Dent. 2015;35 (1):105–14. doi:10.11607/prd.1826.

22. Zhang Y, Tangl S, Huber CD, Lin Y, Qiu L, Rausch-Fan X. Effects of Choukroun's platelet-rich fibrin on bone regeneration in combination with deproteinized bovine bone mineral in maxillary sinus

augmentation: a histological and histomorphometric study. J Craniomaxillofac Surg. 2012;40(4):321–8. doi:10.1016/j.jcms.2011.04.020.

23. Simonpieri A, Choukroun J, Del Corso M, Sammartino G, Dohan Ehrenfest DM. Simultaneous sinus-lift and implantation using microthreaded implants and leukocyte- and platelet-rich fibrin as sole grafting material: a six-year experience. Implant Dent. 2011;20 (1):2–12. doi:10.1097/ID.0b013e3181faa8af.

24. Kobayashi E, Flückiger L, Fujioka-Kobayashi M, Sawada K, Sculean A, Schaller B, Miron RJ. Comparative release of growth factors from PRP, PRF, and advanced-PRF. Clin Oral Investig. 2016;20(9):2353–60. doi:10.1007/s00784-016-1719-1.

25. Lourenço ES, Mourão CFAB, Leite PEC, Granjeiro JM, Calasans-Maia MD, Alves GG. The in vitro release of cytokines and growth factors from fibrin membranes produced through horizontal centrifugation. J Biomed Mater Res A. 2018;106(5):1373–80. doi:10.1002/jbm.a.36346.

26. Lourenço ES, Alves GG, Barbosa RL, Spiegel CN, Melo-Machado RC, Al-Maawi S, Ghanaati S, Mourão CF. Effects of rotor angle and time after centrifugation on the biological in vitro properties of platelet rich fibrin membranes. J Biomed Mater Res. 2021;109:60–8. doi:10.1002/jbm.b.34680.

27. Aizawa H, Tsujino T, Watanabe T, Isobe K, Kitamura Y, Sato A, Yamaguchi S, Okudera H, Okuda K, Kawase T. Quantitative near-infrared imaging of platelets in platelet-rich fibrin (PRF) matrices: comparative analysis of H-PRF, leukocyte-rich PRF, advanced-PRF and concentrated growth factors. Int J Mol Sci. 2020;21(12):4426. doi:10.3390/ijms21124426.

28. Fujioka-Kobayashi M, Miron RJ, Hernandez M, Kandalam U, Zhang Y, Choukroun J. Optimized platelet-rich fibrin with the low-speed concept: growth factor release, biocompatibility, and cellular response. J Periodontol. 2017;88(1):112–21. doi:10.1902/jop.2016.160443.

29. Simões-Pedro M, Tróia PMBPS, Santos NBM, Completo AMG, Castilho RM, Fernandes GVO. Tensile strength essay comparing three different platelet-rich fibrin membranes (L-PRF, A-PRF, and A-PRF+): a mechanical and structural in vitro evaluation. Polymers. 2022;14(7):1392. doi:10.3390/polym14071392.

30. Tsujino T, Masuki H, Nakamura M, Isobe K, Kawabata H, Aizawa H, Watanabe T, Kitamura Y, Okudera H, Okuda K, et al. Striking differences in platelet distribution between advanced-platelet-rich fibrin and concentrated growth factors: effects of silica-containing plastic tubes. J Funct Biomater. 2019;10(3):43. doi:10.3390/jfb10030043.

31. Yüce E, Kömerik N. Potential effects of advanced platelet rich fibrin as a wound-healing accelerator in the management of alveolar osteitis: a randomized clinical trial. Niger J Clin Pract. 2019;22 (9):1189–95. doi:10.4103/njcp.njcp_27_19.

32. To M, Su C, Hidaka K, Okudera T, Matsuo M. Effect of advanced platelet-rich fibrin on accelerating alveolar bone formation in dogs: a histological and immunofluorescence evaluation. Anat Sci Int. 2019;94(3):238–44. doi:10.1007/s12565-019-00479-1.

33. Liu Y-H, To M, Okudera T, Wada-Takahashi S, Takahashi S-S, Su C-Y, Matsuo M. Advanced platelet-rich fibrin (A-PRF) has an impact on the initial healing of gingival regeneration after tooth extraction. J Oral Biosci. 2021;64(1):141–7. doi:10.1016/j-job2021.11.001.

34. Rao JKD, Bhatnagar A, Pandey R, Arya V, Arora G, Kumar J, Bootwala F, Devi WN. A comparative evaluation of iliac crest bone graft with and without injectable and advanced platelet rich fibrin in secondary alveolar bone grafting for cleft alveolus in unilateral cleft lip and palate patients: a randomized prospective study. J Stomatol Oral Maxillofac Surg. 2021;122(3):241–7. doi:10.1016/j.jormas.2020.07.007.

35. Chellathurai BNK, Ganesh B, Rajaram V. Advanced platelet-rich fibrin in periosteal inversion technique for root coverage: a case report. Clin Adv Periodontics. 2020;10(4):181–5. doi:10.1002/cap.10119.

36. Shirakata Y, Sena K, Nakamura T, Shinohara Y, Imafuji T, Setoguchi F, Noguchi K, Kawase T, Miron R. Histological evaluation of gingival and intrabony periodontal defects treated with platelet-rich fibrin using different protocols: a canine study. Oral Health Prev Dent. 2021;19(1):537–46. doi:10.3290/j.ohpd.b2182985.

37. Silva LMP, Sávio DSF, Ávila FC, Vicente RM, Reis GGD, Denardi RJ, Costa NMM, Silva PHF, Mourão CFAB, Miron RJ, et al. Comparison of the effects of platelet concentrates produced by high and low-speed centrifugation protocols on the healing of critical-size defects in rat calvaria: a micromographic and histomorphometric study. Platelets. 2022;19:1–0. doi:10.1080/09537104.2022.2071851.

38. Messora MR, Nagata MJ, Dornelles RC, Bomfim SR, Furlaneto FA, De Melo LG, Deliberador TM, Bosco AF, Garcia VG, Fucini SE. Bone healing in critical-size defects treated with platelet-rich plasma: a histologic and histometric study in rat calvaria. J Periodontal Res. 2008;43(2):217–23. doi:10.1111/j.1600-0765.2007.01017.x.

39. Nagata MJ, Messora M, Pola N, Campos N, Vieira R, Esper LA, Sbrana M, Fucini S, Garcia V, Bosco A. Influence of the ratio of particulate autogenous bone graft/platelet-rich plasma on bone healing in critical-size defects: a histologic and histometric study in rat calvaria. J Orthop Res. 2010;28(4):468–73. doi:10.1002/jor.21027.

40. Mariano R, Messora M, De Morais A, Nagata M, Furlaneto F, Avelino C, Paula F, Ferreira S, Pinheiro M, De Sene JP. Bone healing in critical-size defects treated with platelet-rich plasma: a histologic and histometric study in the calvaria of diabetic rats. Oral Surg Oral Med Oral Pathol Oral Radiol Endod. 2010;109 (1):72–8. doi:10.1016/j.tripleo.2009.08.003.

41. Harkness JE, Wagner JE. Clinical procedures. The biology and medicine of rabbits and rodents. 5th ed. Philadelphia: Williams & Wilkings; 2010. p. 107–94.

42. Hoff J. Methods of blood collection in the mouse. Lab Anim (NY). 2000;29:47–53.

43. Miron RJ, Choukroun J, Ghanaati S. Reply from authors: rE: optimized platelet-rich fibrin with the low-speed concept: growth factor release, biocompatibility, and cellular response: necessity for standardization of relative centrifugal force values in studies on platelet-rich fibrin. J Periodontol. 2019;90(2):122–5. doi:10.1002/JPER.18-0329.

44. Mulinari-Santos G, Santos JS, Palin LP, Silva ACE, Antoniali C, Faverani LP, Okamoto R. Losartan improves alveolar bone dynamics in normotensive rats but not in hypertensive rats. J Appl Oral Sci. 2019;27:e20180574. doi:10.1590/1678-7757-2018-0574.

45. Puttini IO, Gomes-Ferreira PHS, Oliveira D, Hassumi JS, Gonçalves PZ, Okamoto R. Teriparatide improves alveolar bone modelling after tooth extraction in orchiectomized rats. Arch Oral Biol. 2019;102:147–54. doi:10.1016/j.archoralbio.2019.04.007.

46. Ramalho-Ferreira G, Faverani LP, Grossi-Oliveira GA, Okamoto T, Okamoto R. Alveolar bone dynamics in osteoporotic rats treated with raloxifene or alendronate: confocal microscopy analysis. J Biomed Opt. 2015;20(3):038003. doi:10.1117/1.JBO.20.3.038003.

47. Miron RJ, Xu H, Chai J, Wang J, Zheng S, Feng M, Zhang X, Wei Y, Chen Y, Mourão CFAB, et al. Comparison of platelet-rich fibrin (PRF) produced using 3 commercially available centrifuges at both high (~700g) and low (~200g) relative centrifugation forces. Clin Oral Investig. 2020;24(3):1171–82. doi:10.1007/s00784-019-02981-2.

48. Engler-Pinto A, Siéssere S, Calefi A, Oliveira L, Ervolino E, Souza S, Furlaneto F, Messora M. Effects of leukocyte- and platelet-rich fibrin associated or not with bovine bone graft on the healing of bone defects in rats with osteoporosis induced by ovariectomy. Clin Oral Impl Res. 2019;30(10):962–76. doi:10.1111/clr.13503.

49. El Bagdadi K, Kubesch A, Yu X, Al-Maawi S, Orlowska A, Dias A, Booms P, Dohle E, Sader R, Kirkpatrick CJ, et al. Reduction of relative centrifugal forces increases growth factor release within solid platelet-rich fibrin (PRF)-based matrices: a proof of concept of LSCC (low speed centrifugation concept). Eur J Trauma Emerg Surg. 2019;45(3):467–79. doi:10.1007/s00068-017-0785-7.

50. Kobayashi E, Flückiger L, Fujioka-Kobayashi M, Sawada K, Sculean A, Schaller B, Miron RJ. Comparative release of growth factors from PRP, PRF, and advanced-PRF. Clin Oral Invest. 2016;20(9):2353–60. doi:10.1007/s00784-016-1719-1.

51. Dohan Ehrenfest DM, Pinto NR, Pereda A, Jiménez P, Corso MD, Kang BS, Nally M, Lanata N, Wang HL, Quirynen M. The impact of the centrifuge characteristics and centrifugation protocols on the cells, growth factors, and fibrin architecture of a leukocyte- and platelet-rich fibrin (L-PRF) clot and membrane. Platelets. 2018;29 (2):171–84. doi:10.1080/09537104.2017.1293812.

52. Mourão C, Valiense H, Melo R, Mourão NB, Maia MD. Obtention of injectable platelets rich-fibrin (i-PRF) and its polymerization with bone graft: technical note. Rev Col Bras Cir. 2015;42(6):421–3. doi:10.1590/0100-69912015006013.

53. Wend S, Kubesch A, Orlowska A, Al-Maawi S, Zender N, Dias A, Miron RJ, Sader R, Booms P, Kirkpatrick CJ, et al. Reduction of the relative centrifugal force influence cell number and growth factor release within injectable PRF-based matrices. J Mater Sci Mater Med. 2017;28(12):188. doi:10.1007/s10856-017-5992-6.

54. Miron RJ, Bosshardt DD. OsteoMacs: key players around bone biomaterials. Biomaterials. 2015;82:1–19. doi:10.1016/j.biomaterials.2015.12.017.

55. Chang MK, Raggatt L-J, Alexander KA, Kuliwaba JS, Fazzalari NL, Schroder K, Maylin ER, Ripoli VM, Hume DA, Pettit AR. Osteal tissue macrophages are intercalated throughout human and mouse bone lining tissues and regulated osteoblast function in vitro and in vivo. J Immunol. 2008;181(2):1232–44. doi:10.4049/jimmunol.181.2.1232.

56. Batoon L, Millard SM, Raggatt L-J, Pettit AR. Osteomacs and bone regeneration. Curr Osteoporos Rep. 2017;15(4):385–95. doi:10.1007/s11914-017-0384-x.

57. Fujioka-Kobayashi M, Kono M, Katagiri H, Schaller B, Zhang Y, Sculean A, Miron RJ. Histological comparison of platelet rich fibrin clots prepared by fixed-angle versus horizontal centrifugation. Platelets. 2021;32(3):413–9. doi:10.1080/09537104.2020.1754382.

58. Sinder BP, Pettit AR, Mccauley LK. Macrophages: their emerging roles in bone. J Bone Miner Res. 2015;30(12):2140–9. doi:10.1002/jbmr.2735.

59. Winkler IG, Sims NA, Pettit AR, Barbier V, Nowlan B, Helwani F, Poulton TJ, van Rooijen N, Alexander KA, Raggatt LJ, et al. Bone marrow macrophages maintain hematopoietic stem cell (HSC) niches and their depletion mobilizes HSCs. Blood. 2010;116(23):4815–28. doi:10.1182/blood-2009-11-253534.

60. Mourão CF, Lowenstein A, Mello-Machado RC, Ghanaati S, Pinto N, Kawase T, Alves GG, Messora MR. Standardization of animal models and techniques for platelet-rich fibrin production: a narrative review and guideline. Bioengineering. 2023;10:482. doi:10.3390/bioengineering10040482.